Lambda-doublet specificity in the low-temperature capture of NO($X\,^2\Pi_{1/2}$) in low rotational states by C^+ ions

M. Auzinsh,[1] E. I. Dashevskaya,[2,3] I. Litvin,[2,3] E. E. Nikitin,[2,3] and J. Troe[3,4,a)]
[1]*Department of Physics, University of Latvia, Riga LV-1586, Latvia*
[2]*Schulich Faculty of Chemistry, Technion-Israel Institute of Technology, Haifa 32000, Israel*
[3]*Max-Planck-Institut für Biophysikalische Chemie, Am Fassberg 11, Göttingen D-37077, Germany*
[4]*Institut für Physikalische Chemie, Universität Göttingen, Tammannstrasse 6, Göttingen D-37077, Germany*

(Received 25 August 2008; accepted 18 November 2008; published online 6 January 2009)

Following our general approach to Λ-doubling specificity in the capture of dipolar molecules by ions [M. Auzinsh *et al.*, J. Chem. Phys. **128**, 184304 (2008)], we calculate the rate coefficients for the title process in the temperature range $10^{-4}<T<10^2$ K. Three regimes considered are as follows: (i) nonadiabatic capture in the regime of high-field Stark effect with respect to the Λ-doubling components, ($10^{-1}<T<10^2$ K), (ii) adiabatic capture in the regime of intermediate Stark effect ($10^{-3}<T<10^{-1}$ K), and (iii) adiabatic capture in the limit of very low temperatures ($T\ll 10^{-3}$ K) in the regime of quadratic Stark effect with respect to the Λ-doubling and hyperfine components. The results predict a high specificity of the capture rates with respect to the Λ-doublet states even under conditions when the collision energy of the partners strongly exceeds the Λ-doubling splitting. © *2009 American Institute of Physics*. [DOI: 10.1063/1.3043365]

I. INTRODUCTION

There is a growing interest in the dynamic properties of elementary chemical reaction at ultralow temperatures (ULTs). On the one hand, temperatures in the range 10–20 K are relevant for interstellar molecular clouds, i.e., for astrochemical applications.[1–3] On the other hand, efficient cooling techniques for atoms and molecules[4–9] open an access to chemical reactions under sub-Kelvin laboratory conditions.

At ULTs, primarily, barrierless processes are important which are initiated by capture in the long-range part of the interaction potential. Under these conditions, a variety of specific quantum effects may become apparent which would be averaged out at high temperatures. In a series of articles such as Refs. 10–14 we have investigated translational and rotational quantum effects of the reactants.

The present work considers specific low-temperature quantum effects in the capture of diatomic molecules by ions, choosing the capture of NO($X\,^2\Pi_{1/2}$) by C^+ ions as a representative example. It builds on previous theoretical work like Refs. 15–17 and, in particular, on Ref. 18 in which a general discussion of nonadiabatic transitions between Λ-doubling states during the capture process was presented.

The rate coefficient of the capture of NO($X\,^2\Pi_{1/2}$) by C^+ at low temperatures was measured in Ref. 4 at the translational temperature $T=0.6$ K. Initially, it was interpreted in the framework of a simple model that only assumed charge-permanent dipole (cd) interaction. Later it was realized that at this temperature the capture is effected also by the charge-induced dipole (cid) interaction.[15,16] The theoretical value of the capture rate coefficient, calculated for the ground rotational state of NO($X\,^2\Pi_{1/2}, j=1/2$) in the adiabatic channel (AC) treatment of first-order cd and cid interactions, was found to agree with the experimental one within experimental error.[15] Later work[17] revealed that the form of the interaction adopted in Refs. 15 and 16 for the state $j=1/2$ provides only a poor approximation to an accurate AC potential and that the latter is reasonably well represented by a more accurate perturbed rotor (PR) potential which includes, in addition to the first-order cd and the cid interactions, also the second-order cd interaction. This finding cast doubts on the earlier interpretation of the experiment. Indeed, it was found that the theoretical rate coefficient agrees with the experimental one only if the former corresponds to an average of rotationally state-specific rate coefficients at the rotational temperature of about 20 K, i.e., a value also suggested in Ref. 4. It appears that state-specific rate coefficients for the capture of NO($X\,^2\Pi_{1/2}, j$) by C^+ such as calculated in Ref. 17 now provide sufficient information for an interpretation of more detailed experiments, which are not necessarily related to canonical translational and rotational ensembles. One of the possible experiments could be the measurement of a capture rate, or an exothermic charge transfer event, with the participation of a NO($X\,^2\Pi_{1/2}$) molecule in a specified rotational and Λ-doubling state. The feasibility of such an experiment is evident from recent studies of the inelastic scattering of NO and OH on noble gases from a single Λ-doubling component of the ground rotational state.[6–9]

The aim of the present work, in line with the general approach presented in Ref. 18, is the calculation of Λ-doubling state-specific capture rate coefficients for NO($X\,^2\Pi_{1/2}, j, \varepsilon=\pm 1$)+$C^+$. Low-energy (temperature) collisions for $j=1/2$, $j=3/2$, and $j=5/2$ are considered and hyperfine (HF) structure effects are discussed for very low energies (temperatures). Section II describes some general features of the capture dynamics of the title process. In Sec. III, the nonadiabatic (with respect to Λ-doubling states)

a)Electronic mail: shoff@gwdg.de.

TABLE I. Values of relevant parameters for NO($X\ ^2\Pi_{1/2}$).

Parameter	B_{eff}	D_e	ρ
MHz	50 124	0.016	355.2
cm^{-1}	1.67	5.33×10^{-7}	0.0118
K	2.41	7.68×10^{-7}	0.0170

$\mu_D=0.063$ a.u.$=0.16$ D$=1.60\times10^{-19}$ esu cm;
$\alpha=1.680\times10^{-24}$ $\text{cm}^3=11.337$ a.u.;
$Q=-2.421\times10^{-26}$ esu $\text{cm}^2=-1.80$ a.u.

capture in the regime of high-field Stark effect for $j=1/2$, $j=3/2$, and $j=5/2$ states is discussed. Section IV is devoted to adiabatic capture in the regime of intermediate Stark effect. Section V discusses an influence of the HF interaction in the ground state of NO $(j=1/2,\varepsilon=+1)$ in the regime of the quadratic Stark effect. Section VI concludes the article.

II. QUALITATIVE ASPECTS OF THE INTERACTION OF NO($X\ ^2\Pi_{1/2}$) IN LOW ROTATIONAL STATES WITH AN ION

The states of a free, rigid NO molecule in the electronic state $X\ ^2\Pi_{1/2}$ within Hund's coupling case *a*, which belong to the manifold specified by the intrinsic angular momentum quantum number j, are two Λ-doubling components characterized by different molecular parity index $\varepsilon=\pm1$ [or the parity $p=\varepsilon(-1)^{j-1/2}$] and the HF states characterized by the total angular momentum quantum number F. The latter corresponds to the sum $\mathbf{F}=\mathbf{j}+\mathbf{I}$, where $\mathbf{I}$ is the total nuclear spin. In our case, $I=1$ for $^{14}\text{N}^{16}\text{O}$ and $I=1/2$ for $^{15}\text{N}^{16}\text{O}$. The energy levels of the free rotor E_j then are split into several components with the Λ-doubling and HF energy increments $\Delta E^{\Lambda}_{j,\varepsilon}$ and $\Delta E^{\text{HF}}_{j,\varepsilon,I,F}$, respectively. The latter quantities are known with high accuracy, see, e.g., Refs. 19–23. For our purposes, we will use a simplified expression for $\Delta E^{\Lambda}_{j,\varepsilon}$ and corrected values for the rotational energies given in the text of Ref. 24.

$$E_j = B_{\text{eff}} j(j+1) - D_e j^2 (j+1)^2,$$
$$\Delta E^{\Lambda}_{j,\varepsilon} = -\varepsilon \frac{\rho}{2}(j+1/2). \tag{1}$$

Equation (1) contains three molecular parameters, B_{eff}, D_e, and ρ, which are listed in Table I. As far as the quantities $\Delta E^{\text{HF}}_{j,\varepsilon,I,F}$ are concerned, they will be discussed in Sec. V.

The interaction of the NO molecule with an ion at large distances R, which determine the capture at low energies, is composed of charge-permanent dipole, charge-permanent quadrupole (cq), and cid terms. As discussed in Ref. 18, a simplified representation of this interaction contains three parameters, the permanent dipole and quadrupole moments, μ_D and Q, and the isotropic polarizability α, such as also listed in Table I, and is formulated as

$$V(R,\gamma) = \frac{q\mu_D}{R^2}P_1(\cos\ \gamma) + \frac{qQ}{R^3}P_2(\cos\ \gamma) - \frac{q^2\alpha}{2R^4}. \tag{2}$$

The interaction potential of Eq. (2) generates a set of AC potentials calculated from the eigenvalues of the Hamiltonian of a free symmetric dipolar rigid rotor interacting with an ion at a fixed interfragment distance R, or their PR counterparts. The latter are constructed in such a way that they include the terms with the same powers of R as in Eq. (2), i.e., they incorporate first-order cd interaction, first-order cq interaction, and the Langevin (L) interaction [the sum of the cid interaction and the second-order cd interaction].

In constructing adiabatic potentials, it is instructive to discuss different approximations referring to the first term at the right-hand side (rhs) of Eq. (2) that represents the cd interaction. Then, the accurate AC potentials (derived from the Hamiltonian matrix formulated in an extended basis set) would correspond to the multilevel Stark pattern of states that include both high-field and low-field limits. The PR approximation to the AC potentials includes, if the Λ-doubling and HF effects are ignored, the first-order and the second-order cd interactions with respect to the coupling of different rotational states. If Λ-doubling and HF effects are included, the first-order interaction gives rise to an intermediate Stark effect in the manifold of states belonging to each value of j. The limiting cases of this intermediate Stark effect are quadratic or linear Stark effects that correspond, respectively, to the lower or higher values of first-order cd interactions with respect to the HF Λ-doubling spacing within a j-manifold. This nomenclature is the same as used in discussions of the orientation of NO in a uniform electric field.[25] Finally, if the HF interaction is ignored but Λ-doubling is retained, the intermediate Stark effect is reproduced by a two-state model that is parametrized by the first-order cd interaction and the Λ-doubling splitting. This approximation is the dynamical counterpart of the two-level model used in Ref. 25 for the description of the static orientation of NO in an external electric field.

In the light of the above comments, we now consider the hierarchy of approximations for the AC potentials, which will be used in different temperature ranges. This hierarchy is based on the relative magnitude of the rotational constant B, the Λ-doubling spacing for a given j, and the HF splitting for given j,ε. As an example, the values of the three quantities mentioned, for the rotational state $j=1/2$, are (in frequency units) 50 000 MHz (for B), 400 MHz (for the Λ-doubling transition), and 20 MHz (for the $\varepsilon=1,F=1/2\leftrightarrow\varepsilon=1,F=3/2$ transition) (Table II).

TABLE II. Frequencies of the HF Λ-doubling transitions between states F_ε from the manifolds $X\ ^2\Pi_{1/2},j=1/2,\varepsilon=\pm1,I=1/2,1$ (after Ref. 19) of NO.

F_-	F_+	Frequency (MHz)
	$^{14}\text{N}^{16}\text{O}$, $I=1$	
1/2	1/2	205.95
3/2	3/2	431.19
3/2	1/2	411.21
1/2	3/2	225.94
	$^{15}\text{N}^{16}\text{O}$, $I=1/2$	
0	0	501.20
0	1	482.62
1	0	309.22
1	1	290.64

If Λ-doubling effects and HF interaction are ignored, the AC potentials (or their PR counterparts) are written as $V_{\tilde{\Omega},j,m}(R)$ [or $V^{\mathrm{PR}}_{\tilde{\Omega},j,m}(R)$], where $\tilde{\Omega}$ and m are the projections of **j** onto the molecular and collision axes, respectively (exact quantum numbers in the AC approximation) and j is yet another quantum number that specifies the AC potential and which is adiabatically correlated with the quantum of the intrinsic angular momentum of NO. The invariance of the AC potentials with respect to reflection on the plane of the three particles (N, O, and C) implies the symmetry property $V_{\tilde{\Omega},j,m}(R)=V_{-\tilde{\Omega},j,-m}(R)$.

For a fixed value of $\tilde{\Omega}$, the potentials can be labeled by positive and negative values of m (e.g., in Ref. 17 positive values of m were assigned to asymptotically attractive AC potentials, and negative to repulsive ones).

If the Λ-doubling effect is taken into account but the HF interaction is ignored, the AC potentials (or their PR counterparts) are written as $\tilde{V}_{j,\varepsilon,m}(R)$ [or $\tilde{V}^{\mathrm{PR}}_{j,\varepsilon,m}(R)$]. Here, j and ε are AC quantum numbers that adiabatically correlate with the respective quantum numbers of the free molecule. As explained in Ref. 18, the quantities $\tilde{V}_{j,\varepsilon,m}(R)$ [and $\tilde{V}^{\mathrm{PR}}_{j,\varepsilon,m}(R)$] can be recovered from $V_{j,\tilde{\Omega},m}(R)$ [and $V^{\mathrm{PR}}_{j,\tilde{\Omega},m}(R)$] by a simple procedure. For instance, the expression for $\tilde{V}_{j,\varepsilon,m}(R)$ reads

$$\tilde{V}_{j,\varepsilon,m}=\frac{V_{j,\tilde{\Omega},m}+V_{j,\tilde{\Omega},-m}}{2}-\frac{\varepsilon}{2}\sqrt{(V_{j,\tilde{\Omega},m}-V_{j,\tilde{\Omega},-m})^2+(\Delta E^{\Lambda}_j)^2}+\frac{\varepsilon}{2}\Delta E^{\Lambda}_j, \quad (3)$$

where $\Delta E^{\Lambda}_j=\Delta E^{\Lambda}_{j,-1}-\Delta E^{\Lambda}_{j,1}$, see Eq. (1). It can be easily verified that the rhs of Eq. (3) does not depend on the sign of $\tilde{\Omega}$ and the reflection symmetry requires $\tilde{V}_{j,\varepsilon,m}(R)=\tilde{V}_{j,\varepsilon,-m}(R)$. The potentials $V_{j,\tilde{\Omega},m}(R)$ [or $\tilde{V}_{j,\varepsilon,m}(R)$] are formulated relative to the asymptotic energy levels of the free rotor with quantum number j (or j,ε). In the limit of small ΔE^{Λ}_j, when $\Delta E^{\Lambda}_j \ll |V_{j,\tilde{\Omega},m}-V_{j,\tilde{\Omega},-m}|$, the potentials $\tilde{V}_{j,\varepsilon,m}(R)$ are related to $V_{j,\tilde{\Omega},m}(R)$ in the following way:

$$\tilde{V}_{j,\varepsilon,m}(R)|_{\text{small }\Delta E^{\Lambda}_j}=V_{j,|\tilde{\Omega}|,m'}(R)|_{m'=\varepsilon|m|}, \quad (4)$$

provided that the first-order charge-dipole interaction is written as $-|\tilde{\Omega}|m'\mu_D q/R^2$. Within this convention (adopted in Ref. 17), we will write the potentials $V_{j,|\tilde{\Omega}|,m'}(R)$ in a simplified way as $V_{j,m'}(R)$. Note that the appearance of the square root in Eq. (3) corresponds to the intermediate two-state Stark effect with respect to the coupling between different Λ-doubling components of the same j-state, see Sec. IV. The PR counterpart of Eq. (3) reads[18]

$$\tilde{V}^{\mathrm{PR}}_{j,\varepsilon,m}(R)=\tilde{V}^{\mathrm{cd}}_{j,\varepsilon,m}(R)+V^{\mathrm{cq}}_{j,m}(R)+V^{L}_{j,m}(R). \quad (5)$$

Here

$$\tilde{V}^{\mathrm{cd}}_{j,\varepsilon,m}(R)=-\frac{\varepsilon}{2}\sqrt{(\Delta E^{\Lambda}_j)^2+\frac{q^2\mu_D^2m^2}{R^4j^2(j+1)^2}}+\varepsilon\Delta E^{\Lambda}_j/2, \quad (6)$$

$$V^{\mathrm{cq}}_{j,m}(R)=\frac{qQ}{R^3}\frac{(j(j+1)-3m^2)}{(2j+3)(2j-1)}\frac{(j(j+1)-3/4)}{j(j+1)}, \quad (7)$$

$$V^{L}_{j,m}(R)=-\frac{\alpha q^2}{2R^4}\left\{1-\frac{\mu_D^2}{\alpha B}\left(\frac{(j^2-1/4)(j^2-m^2)}{j^3(2j-1)(2j+1)}-\frac{((j+1)^2-1/4))((j+1)^2-m^2)}{(j+1)^3(2j+1)(2j+3)}\right)\right\}. \quad (8)$$

The potentials $\tilde{V}_{j,\varepsilon,m}(R)$ and $V_{j,m'}(R)$, whose limiting forms correspond to the linear (Sec. III) and quadratic (Sec. IV) Stark effects (with respect to the coupling between different Λ-doubling components of the same j-state), are used in these sections for calculating the capture rate coefficients for $j=1/2$, 3/2, and 5/2.

If both the Λ-doubling effect and HF interaction are taken into account, the AC potentials are obtained by diagonalization of the matrix $\tilde{\tilde{\mathbf{V}}}$ that consists of the sum of the matrix **V** corresponding to Eq. (2) and the matrix of the Λ-doubling and HF interactions of a free molecule. The latter matrix is diagonal in the j,ε,I,F,M representation. Besides the quantum numbers j,ε, the respective AC potentials will be labeled by three more quantum numbers, the nuclear spin quantum number I, the projection of the total angular momentum onto the collision axis M, and the additional quantum number that can be called F and which bears the asymptotic significance. Thus, the set of subscripts that specify an AC potential $\tilde{\tilde{V}}_{j,\varepsilon,I,F,M}$ contains asymptotic quantum numbers j,ε,F and exact quantum numbers I,M. In the PR approximation, j becomes a good quantum number. In the limit, when the HF spacing for the free molecule is much larger than the spacing between the AC potentials $\tilde{\tilde{V}}_{j,\varepsilon,I,F,M}$ and $\tilde{\tilde{V}}_{j,\varepsilon,I,F',M'}$ (which happens for very large interpartner distances), the quantum numbers j,ε,F fall into the category of good quantum numbers. This case is discussed in Sec. V for capture with $j=1/2$.

The potentials $\tilde{V}_{j,\varepsilon,m}(R)$ and $\tilde{V}^{\mathrm{PR}}_{j,\varepsilon,m}(R)$ were shown in Figs. 1–3 of Ref. 18. The inspection of these figures indicates a qualitatively different pattern of the AC and PR potentials that is due to the ever-increasing role of the charge-quadrupole interaction in comparison to the decrease in the first-order cd interaction. This feature is illustrated in Fig. 1 where potentials at the left-hand side (lhs) of the diagrams are labeled by $m'=\varepsilon|m|$. The following remarks about the applicability of the PR approximation for the calculation of low-temperature rate coefficients for the capture of $\mathrm{NO}(X\,^2\Pi_{1/2},j,\varepsilon)$ by C^+ therefore should be noted.

(i) For the state $j=1/2$, the PR approximation is applicable for $T<0.5$ K only if the passage over the potential barrier for the AC state $j=1/2,m'=-1/2$ can be ignored. Adiabatic capture then is possible from the lower Λ-component only.

(ii) For the state $j=3/2$, the PR approximation is applicable for $T<0.5$ K only if the AC channel $j=3/2,m'=-1/2$ can be considered as closed (though it does not look like a closed channel in the region of applicability of the PR approximation). Adiabatic capture is possible from the lower Λ-component only if one ignores the incorrect behavior of the PR AC for $j=3/2,m'=-1/2$ in the indicated energy range.

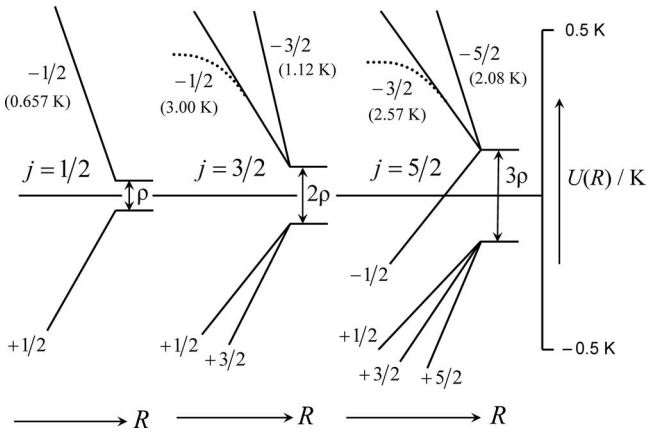

FIG. 1. Qualitative properties of AC potentials (labeled by $m'=\varepsilon|m|$) for NO($X\ ^2\Pi_{1/2},j,\varepsilon$) + ion with $j=1/2$, 3/2, 5/2 and $\varepsilon=-1,1$ in the range of the interaction energy $U/k_B=-0.5\div0.5$ K relative to the mean energy of the Λ-doublet (with HF interaction neglected) vs molecule-ion distance R. Full straight lines schematically stand for the AC PR potentials (first- and second-order multistate Stark effects for charge-dipole interaction). Dotted lines (which deviate from full lines) denote the accurate AC potentials. The Λ-doubling splitting, which increases linearly with j, is strongly enlarged for clarity. The numbers in parentheses show the heights of the accurate potential barriers for initially repulsive AC potentials.

(iii) For the state $j=5/2$, the PR approximation can be used only below 0.1 K if the incorrect behavior of the PR AC potentials does not affect the capture. A novel feature here is the appearance of the attractive AC potential for the $j=5/2, m'=-1/2$ state.

The above features of the AC potentials and their PR counterparts are discussed in detail in Secs. III–V.

III. NONADIABATIC CAPTURE OF NO($X\ ^2\Pi_{1/2}j,\varepsilon$) BY C^+ IN THE HIGH-FIELD STARK REGIME AT $T\gg T_j^\Lambda$

Capture in the high-field Stark regime corresponds to temperatures T that noticeably exceed the characteristic temperatures $T_j^\Lambda=\Delta E_j^\Lambda/k_B$ of the Λ-doubling splitting. Under this condition, the passage of the collision partners over the potential barriers occurs in the region where the Λ-doubling splitting is small in the sense that Eq. (4) applies. Then the effective AC potentials between the molecule and the ion in this region are governed by the AC potentials $V_{j,m'}(R)$. However, during their mutual approach to the barriers, the partners pass a region where the quadratic Stark effect in the potentials $\tilde{V}_{j,\varepsilon,m}(R)$ changes into the linear Stark effect. Nonadiabatic transitions between the AC potentials $\tilde{V}^{\mathrm{PR}}_{j,\varepsilon,m}$ and $\tilde{V}^{\mathrm{PR}}_{j,-\varepsilon,m}$ are possible in this region, and the nonadiabatic transition probability $P_{j,m}$ should be found from the solution of two coupled equations containing the amplitudes of the $|j,\varepsilon,m\rangle^{\mathrm{AC}}$ and $|j,-\varepsilon,m\rangle^{\mathrm{AC}}$ states.[18] Under the condition when the Λ-doubling spacing ΔE_j^Λ is much smaller than the collision energy E, these equations can be formulated in the "impact parameter approximation" (i.e., in the common trajectory approximation for a rectilinear trajectory with a fixed velocity v) of relative motion. The important feature of this approximation is that the probability $P_{j,m}(E)$ depends on a single parameter only,[18] the Massey parameter $\xi_{j,m}$ [i.e., $P_{j,m}(E)=P(\xi_{j,m})$], and, as a consequence, it can be recovered from the probability $P_{1/2,1/2}(E)=P(\xi_{1/2,1/2})$ by the scaling with $\xi_{j,m}=\xi_{1/2,1/2}\sqrt{3m(2j+1)/4j(j+1)}$. The energy dependence of $P_{j,m}(E)$, for j,m states with $j=1/2$, 3/2, and 5/2, is shown in Fig. 2 (only positive m is shown for the pair ε, $-\varepsilon$). In order to demonstrate the validity of the common trajectory approximation, Fig. 2 also shows the values of ΔE_j^Λ on the energy axis. The hatched regions, for the states indicated, correspond to the passage from the adiabatic (to the left from the regions) to the sudden (to the right from the regions) regime with respect to the transition between Λ-doubling states. The inspection of Fig. 2 shows that, for the states under discussion, nonadiabatic capture occurs within the temperature range from tenths to tens of kelvins, and the common trajectory approximation introduced in Ref. 18 is adequate for the calculation of nonadiabatic transition probabilities (this approximation breaks down only when the capture is essentially adiabatic, and the transition probability is negligibly small and, therefore, can be neglected).

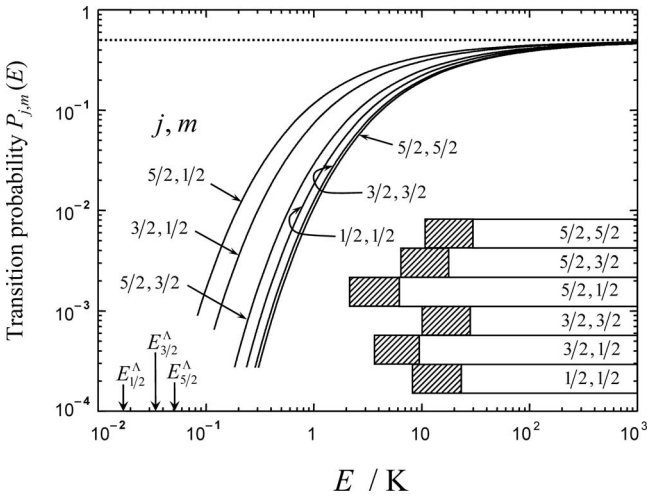

FIG. 2. Nonadiabatic transition probabilities $P_{j,m}$ vs collision energy E for j,m and $j,-m$ AC states (labeled by j,m pairs). The curves are terminated at about $P_{j,m}=10^{-3}$, below which $P_{j,m}$ can be calculated analytically. The arrows indicate the Λ-doubling splitting in the free molecule for $j=1/2$, 3/2, and 5/2. The hatched inserts give the energy ranges where the capture changes from near adiabatic to near sudden.

Reduced Λ-doubling specific rate coefficients, $\tilde{\chi}_{j,\varepsilon}$, for $j=1/2$, 3/2, and 5/2 are calculated following the procedure described in Ref. 18. As before, we express the capture rate coefficients k_{capt} in reduced form $\tilde{\chi}=k_{\mathrm{capt}}/k_L$ relative to the Langevin rate coefficient $k_L=2\pi q\sqrt{\alpha/\mu}$. Explicitly, the $\tilde{\chi}_{j,\varepsilon}$ are represented as a sum of partial rate coefficients $\tilde{\chi}_{j,m'}$:

$$\tilde{\chi}_{j,\varepsilon}=\sum_{m'}\tilde{\chi}_{j,m'}, \tag{9}$$

where again $m'=\varepsilon|m|$. In turn, the $\tilde{\chi}_{j,m'}$ are expressed through survival (surv) and transition (trans) rate coefficients $\chi^{\mathrm{surv/trans}}_{j,m'}$ which are calculated using the probabilities $P^{\mathrm{surv/trans}}_{j,m}$ (which account for the Λ-doubling effect) and the effective AC potentials $U_{j,m'}(R,J)$ (that ignore the Λ-doubling effect). The above is concisely expressed through the following set of equations (see Ref. 18 for details):

$$\tilde{\chi}_{j,m'} = 2\chi^{\mathrm{surv}}_{j,m'} + 2\chi^{\mathrm{trans}}_{j,-m'}, \tag{10}$$

$$\chi^{\mathrm{surv/trans}}_{j,m'} = A(T)\int_0^\infty \frac{JdJ}{2j+1}\int_{U^{\max}_{j,m'}(J)}^\infty P^{\mathrm{surv/trans}}_{j,m}(E) \times \exp(-E/k_{\mathrm{B}}T)\frac{dE}{k_{\mathrm{B}}T}, \tag{11}$$

$$A(T) = \sqrt{\frac{8k_{\mathrm{B}}T}{\pi\mu}}\frac{\pi\hbar^2}{\mu k_{\mathrm{B}}T}\frac{1}{2\pi q}\sqrt{\frac{\mu}{\alpha}}, \tag{12}$$

$$P^{\mathrm{surv}}_{j,m}(E) = 1 - P_{j,m}(E), \qquad P^{\mathrm{trans}}_{j,m}(E) = P_{j,m}(E). \tag{13}$$

The energy $U^{\max}_{j,m'}(J)$ that enters Eq. (11) is defined through the properties of the effective AC potentials, composed of the AC potential and the classical centrifugal energy

$$U_{j,m'}(R,J) = \frac{\hbar^2(J+1/2)^2}{2\mu R^2} + V_{j,m'}(R). \tag{14}$$

In turn, $U^{\max}_{j,m'}(J)$ in Eq. (11) corresponds to the maximum of the effective potential $U_{j,m'}(R,J)$ from Eq. (14) if the latter possesses a barrier, it is equal to zero if $U_{j,m'}(R,J)$ is attractive, and it is infinity if $U_{j,m'}(R,J)$ is repulsive.

In particular, for the states with $j=1/2$, there exists a one-to-one correspondence between ε and m', $\varepsilon=2m'$, such that the expression for $\tilde{\chi}_{1/2,\varepsilon}$ assumes the form

$$\tilde{\chi}_{1/2,\varepsilon} = A(T)\int_0^\infty JdJ\left\{\int_{U^{\mathrm{AC,max}}_{1/2,\varepsilon/2}(J)}^\infty (1 - P_{1/2,1/2}(E)) \times \exp(-E/k_{\mathrm{B}}T)\frac{dE}{k_{\mathrm{B}}T} + \int_{U^{\mathrm{AC,max}}_{1/2,-\varepsilon/2}(J)}^\infty P_{1/2,1/2}(E) \times \exp(-E/k_{\mathrm{B}}T)\frac{dE}{k_{\mathrm{B}}T}\right\}. \tag{15}$$

The results of accurate calculations of $\tilde{\chi}_{1/2,\varepsilon}$ are presented in Fig. 3, along with the effective rate coefficient $\tilde{\chi}^{\mathrm{eff}}_{1/2}$ for the capture from thermally populated Λ-components, and the capture rate coefficient $\chi_{1/2}$ calculated earlier with neglecting the Λ-doubling effects.[18] These are expressed as

$$\tilde{\chi}^{\mathrm{eff}}_{1/2} = \frac{\tilde{\chi}_{1/2,+} + \tilde{\chi}_{1/2,-}\exp(-\Delta E^{\Lambda}_{1/2}/k_{\mathrm{B}}T)}{1+\exp(-\Delta E^{\Lambda}_{1/2}/k_{\mathrm{B}}T)}, \qquad \chi_{1/2} = (\tilde{\chi}_{1/2,+} + \tilde{\chi}_{1/2,-})/2. \tag{16}$$

Here, and in the following, we replace the subscripts $\varepsilon=+1$ and $\varepsilon=-1$ by the signs + and − in order to provide an easy distinction from the values of m and m'. As noted in Ref. 17, the accurate rate coefficients below 10 K are well approximated by their PR counterparts that are given by

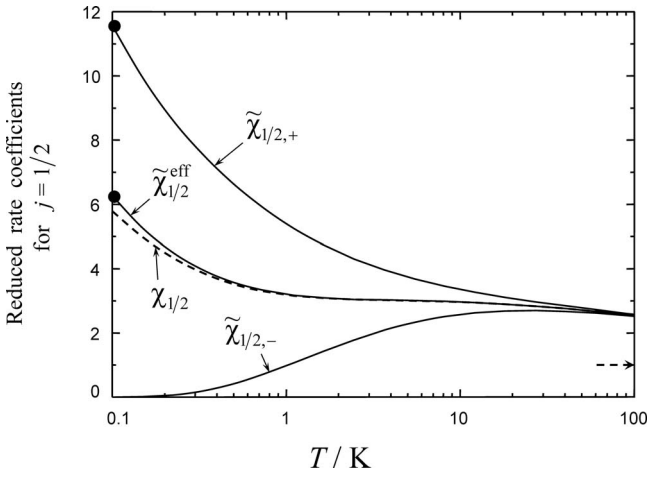

FIG. 3. Capture of NO($^2\Pi_{1/2}, j=1/2, \varepsilon=\pm1$) by C^+ at $T \gg T^{\Lambda}_{1/2}$. Full lines correspond to the accurate reduced rate coefficients $\tilde{\chi}_{1/2,+}$, $\tilde{\chi}_{1/2,-}$, and $\tilde{\chi}^{\mathrm{eff}}_{1/2}$ (for thermal populations of the Λ-components). The dashed line corresponds to the rate coefficient $\chi_{1/2}$ which is the mean of $\tilde{\chi}_{1/2,+}$ and $\tilde{\chi}_{1/2,-}$. The two filled symbols at the lhs correspond to 0.1 K; values for lower T are shown in Figs. 6 and 7. A slight decline of the curves at the rhs of the figure toward the Langevin limit (marked by the arrow) signals the breakdown of the PR approximation.

$$V^{\mathrm{PR}}_{1/2,m'}(R) = -m'\frac{2\mu_D q}{3R^2} - \frac{q^2\alpha^{\mathrm{PR}}}{2R^4}, \tag{17}$$

with the effective PR polarizability $\alpha^{\mathrm{PR}}=\alpha+(4/27)\mu_D^2/B$. When this expression for the potentials is complemented by an approximate analytical expression for $P(E)_{1/2,1/2}$ (see Ref. 18):

$$P_{1/2,1/2}(E) = \frac{\exp(-(c/2)\tilde{J}_{1/2,1/2}\sqrt{\Delta E^{\Lambda}_{1/2}/E})}{1+\exp(-(c/2)\tilde{J}_{1/2,1/2}\sqrt{\Delta E^{\Lambda}_{1/2}/E})}, \tag{18}$$

with the numerical coefficient $c=2.396$ and $\tilde{J}_{1/2,1/2} = (2\mu\mu_D q/3\hbar^2)^{1/2} = 25.62$, the calculation of $\tilde{\chi}^{\mathrm{PR}}_{1/2,\varepsilon}$ becomes quite easy. In particular, as follows from Fig. 2, the capture below 1 K occurs adiabatically with respect to the Λ-doubling states, and, therefore, $\tilde{\chi}_{1/2,\varepsilon}=\tilde{\chi}^{\mathrm{adia}}_{1/2,\varepsilon}$ can be expressed through the partial rate coefficients $\chi_{1/2,m'}$, in which Λ-doubling effects are ignored. Since the latter are well approximated by their PR counterparts and represented analytically,[17] we get, for instance, the following expression for $\tilde{\chi}^{\mathrm{adia}}_{1/2,+}$ over the range $T^{\Lambda}_{1/2} \ll T < 0.1$ K:

$$\tilde{\chi}^{\mathrm{adia}}_{1/2,+}(T) \approx 2\chi^{\mathrm{PR}}_{1/2,1/2} = 2\sqrt{\frac{\alpha^{\mathrm{PR}}}{\alpha}}\left[\frac{1}{6}\sqrt{\frac{2\mu_D^2}{\pi\alpha^{\mathrm{PR}}k_{\mathrm{B}}T}} + \frac{1}{2}\right]. \tag{19}$$

Toward the high-temperature side of the graphs in Fig. 3, the quantities $\tilde{\chi}^{\mathrm{eff}}_{1/2}$ and $\tilde{\chi}^{\mathrm{PR}}_{1/2}$ level off at a temperature of about 10 K which indicates that the capture mainly occurs when the attractive potential is proportional to R^{-4}. This potential differs from the ion-induced dipole potential $-q^2\alpha/2R^4$ because it also contains second-order corrections from the cd interaction. The leveling-off then occurs at values above the true high-temperature limit which is unity. At the low-temperature side, $\tilde{\chi}^{\mathrm{eff}}_{1/2}$ and $\chi_{1/2}$ slightly deviate from each other due to the thermal population factor $\exp(-\Delta E^{\Lambda}_j/k_{\mathrm{B}}T)$.

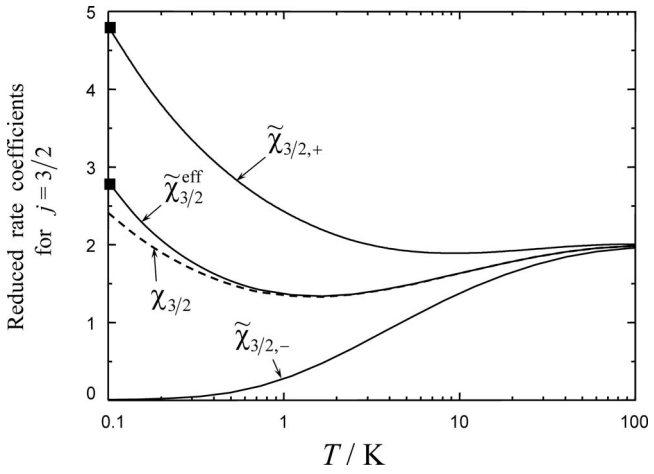

FIG. 4. Capture of NO($^2\Pi_{1/2}, j=3/2, \varepsilon=\pm1$) by C^+ at $T \gg T^{\Lambda}_{3/2}$. Full lines correspond to the accurate reduced rate coefficients, $\tilde{\chi}_{3/2,+}$, $\tilde{\chi}_{3/2,-}$, and $\tilde{\chi}^{\rm eff}_{3/2}$ (for thermal populations of the Λ-components). The dashed line corresponds to the rate coefficient $\chi_{3/2}$ which is the mean of $\tilde{\chi}_{3/2,+}$ and $\tilde{\chi}_{3/2,-}$. The shallow minimum for $\tilde{\chi}_{3/2,+}$, $\tilde{\chi}^{\rm eff}_{3/2}$, and $\tilde{\chi}^{\rm sudd}_{3/2}$ results from the interplay of the charge-dipole and charge-quadrupole interaction. The two filled symbols at the lhs of this figure correspond to 0.1 K; values for lower T are shown in Fig. 7.

A small difference between $\tilde{\chi}^{\rm eff}_{1/2}$ and $\chi_{1/2}$, of course, does not imply that the capture is close to the sudden limit.

For other states ($j=3/2$ and 5/2), the PR approximation is only applicable at substantially lower temperatures, and the calculations of $\tilde{\chi}_{3/2,\varepsilon}$ and $\tilde{\chi}_{5/2,\varepsilon}$ should be based on the accurate AC potentials. Figures 4 and 5 present the graphs of $\tilde{\chi}_{j,\varepsilon}$ for the temperature range $0.1<T<100$ K such as calculated with accurate AC potentials $V_{j,m'}(R)$ and accurate transition probabilities. Also shown are χ_j and the effective rate coefficients $\tilde{\chi}^{\rm eff}_j$ that are defined similar to Eq. (16). Compared to $j=1/2$, a qualitatively new feature for $j=3/2$ is the passage of the rate coefficients through minima. This is due to the interplay of a weaker charge-dipole interaction with the charge-quadrupole interaction which is absent in the case $j=1/2$. An even more drastic difference is observed

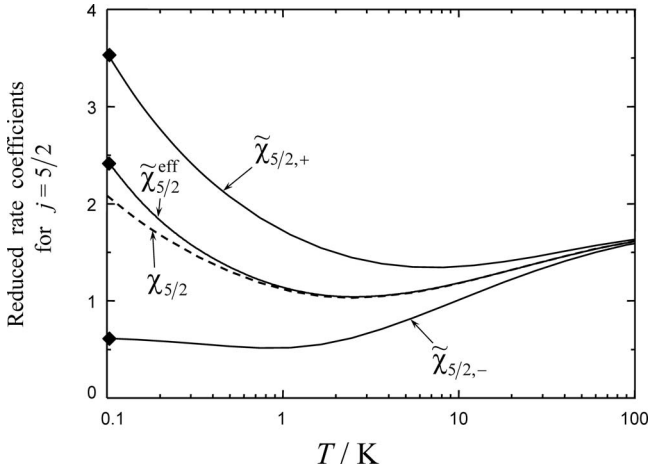

FIG. 5. Capture of NO($^2\Pi_{1/2}, j=5/2, \varepsilon=\pm1$) by C^+ at $T \gg T^{\Lambda}_{5/2}$. Full lines correspond to the accurate reduced rate coefficients, $\tilde{\chi}_{5/2,+}$, $\tilde{\chi}_{5/2,-}$, and $\tilde{\chi}^{\rm eff}_{5/2}$ (for thermal populations of the Λ-components). The dashed line corresponds to the rate coefficient $\chi_{5/2}$ which is the mean of $\tilde{\chi}_{5/2,+}$ and $\tilde{\chi}_{5/2,-}$. The minimum for $\tilde{\chi}_{5/2,+}$, $\tilde{\chi}_{5/2,-}$, and $\tilde{\chi}^{\rm sudd}_{5/2}$ results from the interplay of the charge-quadrupole and weak charge-dipole interaction. The filled symbols at the lhs of this figure correspond to 0.1 K; values for lower T are shown in Fig. 7.

when one compares cases $j=3/2$ and $j=5/2$. In the latter case, due to the relatively larger effect of the charge-quadrupole interaction, the capture from the upper Λ-component becomes possible at lower temperatures. The common important feature for all three cases is that, at temperatures below 1 K which still is much higher than the characteristic temperature for the Λ-doubling splitting, the capture from individual Λ-doubling states occurs adiabatically. This allows one to treat the capture below 1 K within the standard AC approach using AC potentials that explicitly take into account the Λ-doubling splitting.

IV. ADIABATIC CAPTURE OF NO($X\,^2\Pi_{1/2}j,\varepsilon$) BY C^+ IN THE INTERMEDIATE STARK EFFECT REGIME

In the intermediate Stark effect regime, capture occurs under adiabatic conditions. It then follows that, for $T<0.1$ K and $j=1/2$ and 3/2, the capture occurs only from the lower Λ-component ($\varepsilon=+1$) while, for $j=5/2$, beside the capture channels with $m'=1/2$, 3/2, and 5/2 correlating with the $\varepsilon=+1$ state, there exists a channel with $m'=-1/2$ that correlates with the upper Λ-component ($\varepsilon=-1$). For $T<0.1$ K, one can use PR potentials $\tilde{V}^{\rm PR}_{j,\varepsilon,m}(R)$ from Eq. (5). The capture rate coefficient for the AC PR potential in the adiabatic regime assumes the standard form. Explicitly, the $\tilde{\chi}_{j,\varepsilon}$ are represented as a sum of partial rate coefficients $\tilde{\chi}_{j,\varepsilon,m}$ [see Eq. (9)], and the latter are identified with partial adiabatic capture rate coefficients

$$\tilde{\chi}^{\rm PR}_{j,\varepsilon,m} = A(T)\int_0^{\infty} \frac{JdJ}{2j+1} \int_{\tilde{U}^{\rm PR,max}_{j,\varepsilon,m}(J)}^{\infty} \exp(-E/k_{\rm B}T)\frac{dE}{k_{\rm B}T}. \tag{20}$$

Here $\tilde{U}^{\rm PR\ max}_{j,\varepsilon,m}(J)$ is the maximum of the effective potential

$$\tilde{U}^{\rm PR}_{j,\varepsilon,m}(R,J) = \frac{\hbar^2(J+1/2)^2}{2\mu R^2} + \tilde{V}^{\rm PR}_{j,\varepsilon,m}(R). \tag{21}$$

Again we start with the case $j=1/2$ since it is simplest because the first-order charge-quadrupole interaction vanishes. Then the attractive potential $\tilde{V}^{\rm PR}_{1/2,+,1/2}$ collapses into its simplified version

$$\tilde{V}^{\rm PR}_{1/2,+,1/2}(R) = -\frac{1}{2}\sqrt{\left(\frac{2\mu_D q}{3R^2}\right)^2 + (\Delta E^{\Lambda}_{1/2})^2} - \frac{q^2\alpha^{\rm PR}}{2R^4} + \frac{1}{2}\Delta E^{\Lambda}_{1/2}. \tag{22}$$

As argued in Ref. 18, the rate coefficient for capture in the field of the potential of Eq. (22) can be related to $\chi^{\rm PR}_{1/2,+}$ through a damping function $F(T^{\Lambda}_{1/2}/T)$, i.e.,

$$\tilde{\chi}^{\rm PR}_{1/2,+}(T) \approx \tilde{\chi}^{\rm PR,app}_{1/2,+} = 2\chi^{\rm PR}_{1/2,1/2}(T)F(T^{\Lambda}_{1/2}/T), \tag{23}$$

where $\chi^{\rm PR}_{1/2,1/2}(T)$ is defined by Eq. (19) and

$$F(x) = \int_0^1 dy\, \exp[-(x/2)(1-\sqrt{1-y^2})]. \tag{24}$$

The function $F(T^{\Lambda}_{1/2}/T)$ has the asymptotic behavior

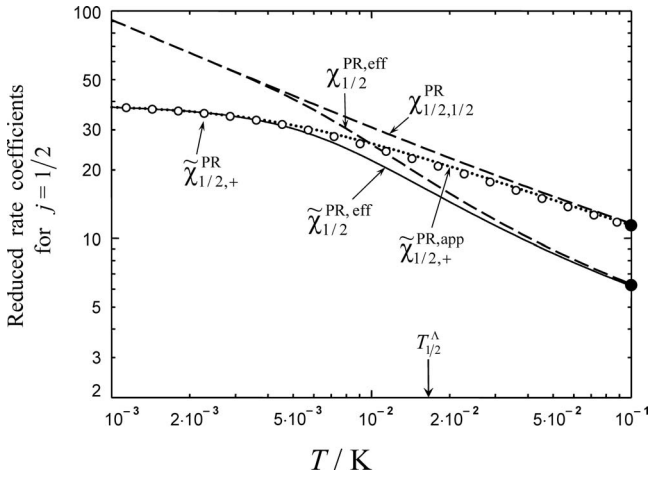

FIG. 6. Capture of NO($^2\Pi_{1/2}, j=1/2, \varepsilon=+1$) by C^+ in the region around $T \approx T^{\Lambda}_{1/2}$ (marked by the arrow). The symbols correspond to the accurate PR rate coefficient $\tilde{\chi}^{\mathrm{PR}}_{1/2,+}$, the full line to $\tilde{\chi}^{\mathrm{PR,eff}}_{1/2}$, and the dots to $\tilde{\chi}^{\mathrm{PR,app}}_{1/2,+}$. The dashed lines correspond to the extrapolations of $\chi^{\mathrm{PR}}_{1/2,+}$ and $\chi^{\mathrm{PR,eff}}_{1/2}$ from $T \gg T^{\Lambda}_{1/2}$ to lower temperatures. The two filled symbols at the rhs of this figure correspond to those at the lhs of Fig. 3.

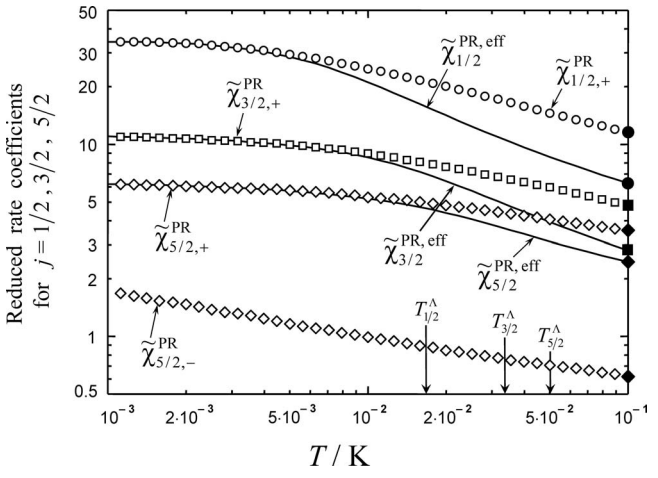

FIG. 7. Capture of NO($^2\Pi_{1/2}, j, \varepsilon=\pm 1$) by C^+ in the region around $T \approx T^{\Lambda}_{j}$ (marked by the arrows) for $j=1/2, 3/2, 5/2$. The open symbols correspond to the reduced rate coefficients $\tilde{\chi}^{\mathrm{PR}}_{j,\varepsilon}$, and the full lines represent $\tilde{\chi}^{\mathrm{PR,eff}}_{j,\varepsilon}$. The filled symbols at the rhs of this figure correspond to those at the lhs of Figs. 3–5.

$$F(x) = \begin{cases} 1, & x \ll 1 \\ \sqrt{\pi/x}, & x \gg 1 \end{cases} \tag{25}$$

and brings the rate $\tilde{\chi}^{\mathrm{PR,app}}_{1/2,+}$ to a constant limit $\tilde{\chi}^{\mathrm{cd},L}_{1/2,+}$ at very low temperatures ($T \ll T^{\Lambda}_{1/2}$) which is appropriate for the cd Langevin interaction $\tilde{V}^{\mathrm{cd},L}_{1/2,+}$:

$$\tilde{V}^{\mathrm{cd},L}_{1/2,+} = -\frac{q^2 \tilde{\alpha}^{\mathrm{cd}}}{2R^4}, \quad \tilde{\alpha}^{\mathrm{cd}} = 2(\mu_D)^2/9\Delta E^{\Lambda}_{1/2},$$
$$\tilde{\chi}^{\mathrm{cd},L}_{1/2,+} = \sqrt{\tilde{\alpha}^{\mathrm{cd}}/\alpha} = 37.2, \tag{26}$$

where the superscript cd means that the polarizability $\tilde{\alpha}^{\mathrm{cd}}$ comes from the second-order Stark effect with respect to the cd interaction mixing the two components of the Λ-doublet. As discussed in Ref. 18, the approximate expression $\tilde{\chi}^{\mathrm{PR,app}}_{1/2,+}(T)|_{T \ll T^{\Lambda}_{1/2}}$ differs from the accurate one $\tilde{\chi}^{\mathrm{PR}}_{1/2,+}(T)|_{T \ll T^{\Lambda}_{1/2}}$ by a relative correction $\alpha^{\mathrm{PR}}/2\tilde{\alpha}^{\mathrm{cd}}$ which is small unless the dipole moment is anomalously low.

Figure 6 shows the plots of the rate coefficients $\tilde{\chi}^{\mathrm{PR}}_{1/2,+}$ (symbols) as well as the approximate expressions $\tilde{\chi}^{\mathrm{PR,app}}_{1/2,+}$ and $\tilde{\chi}^{\mathrm{PR,eff}}_{1/2}$. For comparison, plots of extrapolated values of $\chi^{\mathrm{PR}}_{1/2,1/2}$ and $\chi^{\mathrm{PR,eff}}_{1/2}$ are also shown. At the rhs of this figure, the damping is negligible and the graphs coalesce to two filled circles that correspond to those at the lhs of Fig. 3. At the lhs of Fig. 6, both $\chi^{\mathrm{PR}}_{1/2,1/2}$ and $\chi^{\mathrm{PR,eff}}_{1/2}$ diverge as $T^{-1/2}$ while $\tilde{\chi}^{\mathrm{PR}}_{1/2,+}$ and $\tilde{\chi}^{\mathrm{PR,eff}}_{1/2}$ tend to a limit that approximately corresponds to $\sqrt{\tilde{\alpha}/\alpha}$. We also note that the approximation of Eq. (23) performs quite satisfactorily.

For higher values of j, the capture rate coefficients were calculated using the full AC PR potentials from Eqs. (5)–(8). The comparison of the graphs presented in Fig. 7 shows that $\tilde{\chi}^{\mathrm{PR}}_{3/2,+}$ is noticeably lower than $\tilde{\chi}^{\mathrm{PR}}_{1/2,+}$. This is ascribed to a much weaker charge-dipole interaction which arises from two effects: the smaller value of the dipole moment in the state $j=3/2$ and the stronger suppression of the cd interaction in the intermediate Stark effect regime because of the larger value of the Λ-doubling splitting. These effects become even more pronounced for $j=5/2$. A new feature appears here, the capture from the upper component of the Λ-doublet. The nonzero value of $\tilde{\chi}^{\mathrm{PR}}_{5/2,-}$ is the reflection of the competition between the attractive first-order charge-quadrupole interaction and the repulsive cd interaction in the intermediate Stark effect regime. A noticeable negative temperature dependence of $\tilde{\chi}^{\mathrm{PR}}_{5/2,-}$ signals the prevailing influence of the charge-quadrupole interaction that manifests itself in the incipient $T^{-1/6}$ divergence of the classical rate which is quenched in the quantum regime, see Sec. V.

V. ADIABATIC CAPTURE OF NO($X\,^2\Pi_{1/2} j=1/2$) BY C^+ IN THE QUADRATIC STARK EFFECT REGIME FOR HYPERFINE Λ-DOUBLING STATES

The derivation of the capture rate coefficients in Secs. II–IV ignored the HF structure. However, when the capture occurs at such low temperatures that the thermal energy is comparable to the HF structure splitting, the calculation of the rate coefficients should be based on PR AC potentials that include both the Λ-doubling and the HF interaction. Here, one can anticipate to find a noticeable $^{14}N/^{15}N$ isotope effect that comes from the difference in the structure of the HF Λ-doubling states of $^{14}N^{16}O$ and $^{15}N^{16}O$. An isotope effect of this kind may be expected to be substantially stronger than that arising from the change in the reduced mass of the colliding partners NO+C and the change in the rotational constant of NO.

The PR potentials, $\tilde{\tilde{V}}^{\mathrm{PR}}_{j,\varepsilon,I,F,M}$, can be found by the numerical diagonalization of the energy matrix with the diagonal elements $\Delta E^{\Lambda}_{j,\varepsilon} + \Delta E^{\mathrm{HF}}_{j,\varepsilon,I,F}$ and off-diagonal elements derived from the potentials $V^{\mathrm{PR}}_{j,m'}(R)$ by transforming them from the j,m',I,M_I representation to the j,I,F,M representation.[26] Rather than performing accurate calculations of the potentials $\tilde{\tilde{V}}^{\mathrm{PR}}_{j,\varepsilon,I,F,M}$ in general, we here consider the case $j=1/2$, for which the first-order cq interaction vanishes. This allows one to study the Langevin limit (attractive interaction propor-

tional to R^{-4}) when the potential corresponds to the sum of the second-order charge-permanent dipole, cd, interaction with respect to the HF Λ-doubling spacing (i.e., the quadratic Stark effect), the second-order cd interaction with respect to the spacing between rotational levels, and the cid interaction. Unless the dipole moment is anomalously small, the first interaction is by far the largest, and therefore we consider the attractive potentials $\tilde{\tilde{V}}^{\mathrm{cd},L}_{j,\varepsilon,I,F,M}|_{j=1/2,\varepsilon=+1}=\tilde{\tilde{V}}^{\mathrm{cd},L}_{1/2,+,I,F,M}$. The explicit expression for the latter can be recovered from a general expression for the energy levels of quadratic Stark effect as[27]

$$\tilde{\tilde{V}}^{\mathrm{cd},L}_{j,\varepsilon,I,F,M}(R)=-\frac{q^2(\mu_D)^2}{R^4 16j^2(j+1)^2\Delta E^{\Lambda}_j}G_{j,\varepsilon,I,F,M}, \tag{27}$$

$$G_{j,\varepsilon,I,F,M}=\left\{\frac{\Delta E^{\Lambda}_j M^2[j(j+1)+F(F+1)-I(I+1)]^2}{(E_{j,\mp\varepsilon,I,F}-E_{j,\pm\varepsilon,I,F})F^2(F+1)^2}+\frac{\Delta E^{\Lambda}_j(F^2-M^2)(F+j+I+1)(j-F+I+1)(F-j+I)(j+F-I)}{(E_{j,\mp\varepsilon,I,F-1}-E_{j,\pm\varepsilon,I,F})F^2(2F+1)(2F-1)}\right.$$
$$\left.+\frac{\Delta E^{\Lambda}_j((F+1)^2-M^2)(F+j+I+2)(j-F+I)(F-j+I+1)(j+F+1-I)}{(E_{j,\mp\varepsilon,I,F+1}-E_{j,\pm\varepsilon,I,F})(F+1)^2(2F+3)(2F+1)}\right\}, \tag{28}$$

where $E_{j,\pm\varepsilon,I,F}$ are the energies of the HF Λ-doubling levels, and the quantity ΔE^{Λ}_j was introduced artificially to make the $G_{j,\varepsilon,I,F,M}$ coefficients dimensionless. When one inserts $j=1/2$ into Eq. (27), one rewrites

$$\tilde{\tilde{V}}^{\mathrm{cd},L}_{1/2,+,I,F,M}(R)=\tilde{V}^{\mathrm{cd},L}_{1/2,+}(R)G_{1/2,+,I,F,M}, \tag{29}$$

where $\tilde{V}^{\mathrm{cd},L}_{1/2,+}(R)$ is the cd-L potential in the absence of HF interaction [see Eq. (26)]. If one also puts all energy differences in denominators in Eq. (28) equal to ΔE^{Λ}_j, one finds, as expected, $G_{1/2,+,I,F,M}=1$. It is seen from Eq. (29) that the rate coefficients $\tilde{\tilde{\chi}}^{\mathrm{cd},L}_{1/2,+,I,F,M}$ for the capture by HF Λ-doubling potential are related to the rate coefficients $\tilde{\chi}^{\mathrm{cd},L}_{1/2,+}$ for the capture by a Λ-doubling potential with vanishing HF structure through numerical coefficients $G_{1/2,+,I,F,M}$ as

$$\tilde{\tilde{\chi}}^{\mathrm{cd},L}_{1/2,+,I,F,M}=\tilde{\chi}^{\mathrm{cd},L}_{1/2,+}\sqrt{G_{1/2,+,I,F,M}}, \tag{30}$$

where I equals 1 or 1/2 for $^{14}N^{16}O$ or $^{15}N^{16}O$, and F assumes the values 1/2 and 3/2 or 0 and 1, respectively. Taking transition energies from Tables XII and XIII of Ref. 19, and, for simplicity, writing $G_{j,\varepsilon,I,F,M}|_{j=1/2,\varepsilon=+1,I=1,1/2}\equiv {}^{14,15}G_{F,M}$ we find the following values of the coefficients: $^{14}G_{1/2,1/2}=0.959$, $^{14}G_{1,3/2,1/2}=1.489$, $^{14}G_{3/2,3/2}=0.824$, $^{15}G_{0,0}=1.148$, $^{15}G_{1,0}=0.736$, and $^{15}G_{1,1}=1.222$. With these values of G, the scaled reduced partial capture rate coefficients defined by Eq. (30) are presented in Table III. As follows from Table III, the effective scaled reduced rate coefficient for $^{14}N^{16}O$ with equal populations of two HF levels $F=3/2$ and $F=1/2$ amounts to 1.036 and it increases to 1.064 for the case of prevailing population of the lower HF state (with $F=3/2$). For $^{15}N^{16}O$, the respective values are 1.035 and 1.071 (the lower HF state corresponds to $F=0$). We see that, first, the capture rate coefficients calculated with HF interaction taken into account deviate from those with HF interaction neglected by several percent, and, second, the isotope effect in the scaled rate coefficients amounts to about 1%, with the capture rate for $^{15}N^{16}O$ being higher. Note that this isotope effect is not related to the change in the reduced mass, which does not appear in the scaled rate coefficients. We also mention that a rather weak effect of the HF interaction on the capture rate parallels the conclusion reached in Ref. 25 about a weak effect of the HF interaction on the orientation of the $NO(X\,^2\Pi_{1/2},j=1/2)$ in an external electric field.

TABLE III. Scaled reduced partial capture rate coefficients $^{14,15}\tilde{\tilde{\chi}}^{\mathrm{cd},L}_{1/2,+,F,M}/\tilde{\chi}^{\mathrm{cd},L}_{1/2,+}=\sqrt{{}^{14,15}G_{F,M}}$ for the capture of $^{14,15}N^{16}O(X\,^2\Pi_{1/2}, j=1/2,\varepsilon=+1,F,M)$ by an ion.

$^{14}N^{16}O$		$^{15}N^{16}O$	
F,M	$\sqrt{{}^{14}G_{F,M}}$	F,M	$\sqrt{{}^{15}G_{F,M}}$
1/2, 1/2	0.979	0, 0	1.071
3/2, 1/2	1.220	1, 0	0.858
3/2, 3/2	0.908	1, 1	1.105

The extrapolation of the expressions in Eq. (30) to zero temperature requires a generalization of the AC approach in two respects: for ULTs of the order of $T_{\mathrm{ULT}}=\hbar^4/k_{\mathrm{B}}q^2\tilde{\alpha}^{\mathrm{cd}}\mu^2$ and below, one has to take into account the quantum character of the relative motion (quantization of the total angular momentum, tunneling through and reflection from centrifugal barriers)[10] and the Coriolis coupling between AC states with different values of M, see Ref. 12. The zero-temperature (Bethe) limit of the rate coefficients will exceed the Langevin limit for the case of a single AC potential converging to the limits $F=0$ or $F=1/2$ by a factor of 2 (the Vogt–Wannier[28] result, see also Ref. 10). The qualitative character of the temperature dependence of the rates within the range $T_{\mathrm{ULT}}<T<T^{\Lambda}_{1/2}$ can be inferred by expressing T_{ULT} through the parameters of the problem under discussion. Substituting $\tilde{\alpha}^{\mathrm{cd}}$ from Eq. (26) into the expression for T_{ULT}, we find $T_{\mathrm{ULT}}\approx 2\Delta E^{\Lambda}_{1/2}/k_{\mathrm{B}}\tilde{J}^4_{1/2,1/2}=2T^{\Lambda}_{1/2}/\tilde{J}^4_{1/2,1/2}$. Since $\tilde{J}\gg 1$ (see Sec. III), we see that the quantum regime in the capture occurs much below the characteristic temperature $T^{\Lambda}_{1/2}$ corresponding to the Λ-doubling, and therefore the plots of the functions $\tilde{\tilde{\chi}}^{\mathrm{PR}}_{1/2,\varepsilon,F,M}(T)$ will exhibit a wide plateau within the range $T_{\mathrm{ULT}}<T<T^{\Lambda}_{1/2}$ [as given by Eq. (30)], before they turn up, at $T<T_{\mathrm{ULT}}$, to their zero-temperature limits.

When one passes from $j=1/2$ to higher j, one notes that

the limit similar to $\chi^{\mathrm{PR,L}}_{j,\varepsilon,F,M}$ in Eq. (30), strictly speaking, does not exist since the cq interaction results in a steady increase in the capture rate with decreasing temperature, featuring a $T^{-1/6}$ dependence. Similarly, the wide plateau in the range $T_{\mathrm{ULT}}<T<T_j^{\Lambda}$ is replaced by a curve with a negative slope. However, the Bethe limit still exists which, beside $\tilde{\alpha}^{\mathrm{cd}}$, also depends on Q. The question of the temperature dependence of $\chi^{\mathrm{PR},L}_{j,\varepsilon,F,M}$ for $j>1/2$ in the range $T<T_j^{\Lambda}$ down to zero temperature will be discussed elsewhere.[29]

VI. DISCUSSION AND CONCLUSION

The capture of NO in the lowest rotronic states $X\,^2\Pi_{1/2},j,\varepsilon$ ($j=1/2$, 3/2, and 5/2; $\varepsilon=\pm 1$) by C^+ demonstrates general features of low-temperature complex formation in collisions of a dipolar molecule in a degenerate electronic state with an ion: the state-specific rate coefficients strongly depend on the Λ-doubling state even under conditions when the translational temperature T is much higher than the characteristic temperature T_j^{Λ} of the Λ-doubling splitting. This feature is a consequence of the very slow variation in the perturbation exerted on the molecule by the electric field of the ion upon mutual approach of the partners across the region of the intermediate Stark effect. With decreasing temperature, but for T still higher than T_j^{Λ}, the capture occurs adiabatically with respect to transitions between AC potentials correlating with different Λ-doubling components. Under this condition, the capture from the upper Λ-doubling component does not occur at all for $j=1/2$ and $j=3/2$, but it does occur for $j=5/2$. The qualitative difference between these two cases is due to the subtle interplay between the charge-dipole interaction in the intermediate Stark effect and the charge-quadrupole interaction. This difference demonstrates what happens when the projection of the permanent dipole moment onto the intrinsic angular momentum vector **j** becomes small as a result of the rotational averaging of the dipole moment with an increase in **j**. The capture rate coefficient from the lower Λ-doubling component is quenched compared to its purely cd (linear Stark effect) counterpart and, in the limit of very low temperature, at $T\ll T_j^{\Lambda}$, the rate coefficient is determined by the interaction consisting of a Langevin-type term coming from the second-order Stark effect of the molecular dipole in the external field of the ion (proportional to R^{-4}) and of the charge-quadrupole term (proportional to R^{-3}). For $j=1/2$, the inclusion of the HF interaction neither drastically modifies the qualitative picture of the temperature dependence of the rate coefficients nor the nonadiabatic/adiabatic capture dynamics since the electric field of the ion does not couple HF structure states belonging to the same Λ-doubling component. The rate coefficients at ULTs, when the relative motion of partners shows quantum features, show the familiar approach toward the Vogt–Wannier zero-temperature limit. However, the capture dynamics here is complicated by the fact that the Coriolis coupling tends to average the first-order charge-quadrupole interaction proportional to R^{-3} (effective for higher temperatures). As a result, the consequence of the charge-quadrupole interaction appears in second order (with respect to the states of the relative rotation of the partners) as terms proportional to R^{-4}, see Ref. 12. Thus, the overall potential, which is responsible for the capture in the ULT regime, behaves again like an effective Langevin interaction. On the whole, one can say that the apparent low-temperature divergence of the capture rate coefficients of dipolar and quadrupolar molecules in open electronic state by an ion with decreasing temperature is removed by two effects in succession: first, the $T^{-1/2}$ divergence from the cd interaction is removed by the nonadiabatic rotronic coupling between the adiabatic $X\,^2\Pi_{1/2}$ and $A\,^2\Sigma$ electronic states (which results in the Λ-doubling) and, second, the $T^{-1/6}$ divergence from the cq interaction is removed by the nonadiabatic rotational coupling which manifests itself in the averaging of the first-order cq interaction to zero and the appearance of a modified cd interaction proportional to R^{-4}. As a result, the state-specific HF Λ-doubling capture rate coefficients tend to constant values at zero temperature (the Bethe limit) corresponding to an effective Langevin interaction which incorporates the quadratic Stark effect for the cd interaction, the modified charge-quadrupole interaction, and the cid interaction.

ACKNOWLEDGMENTS

Financial support of this work by the EU Human Potential MCRTIN Contract No. 512302 "The Molecular Universe" is gratefully acknowledged. E.E.N. also acknowledges the support by the award from the Alexander von Humboldt Foundation.

APPENDIX: GLOSSARY OF ABBREVIATIONS USED IN THIS PAPER

AC is the adiabatic channel, PR is the perturbed rotor, cd is the charge-permanent dipole, L is the Langevin, and HF is the hyperfine.

$\chi_{j,m}$ and χ_j are reduced partial (j,m-specific) and total (j-specific) AC capture rate coefficients calculated with Λ-doubling effects and HF interaction ignored (i.e., corresponding to a sudden transition between the HF Λ components). With the PR superscript, the rate coefficients $\chi^{\mathrm{PR}}_{j,m}$ and χ^{PR}_j correspond to AC PR potentials. With PR replaced by cd, the rate coefficients $\chi^{\mathrm{cd}}_{j,m}$ and χ^{cd}_j correspond to the cd interaction in the linear Stark effect regime.

$\chi^{\mathrm{surv/trans}}_{j,m'}$ are reduced auxiliary capture rate coefficients corresponding to survival on a j,m' AC potential and transition to $j,-m'$ potentials for the motion across the nonadiabaticity region.

$\tilde{\chi}_{j,m}$ and $\tilde{\chi}_{j,\varepsilon}$ are reduced partial (j,m-specific) and total (j,ε-specific) capture rate coefficients calculated with Λ-doubling effects taken into account.

$\tilde{\chi}^{\mathrm{PR}}_{j,\varepsilon,F,M}$ are the reduced partial AC PR capture rate coefficients calculated with Λ-doubling and HF effects taken into account.

[1] E. Herbst, J. Phys. Chem. A **109**, 4017 (2005).
[2] H. Sabbah, L. Biennier, I. R. Sims, Yu. Georgievskii, S. J. Klippenstein, and I. W. M. Smith, Science **317**, 102 (2007).
[3] I. W. M. Smith, A. M. Sage, N. M. Donahue, E. Herbst, and D. Quan, Faraday Discuss. **133**, 137 (2006).
[4] T. L. Mazely and M. A. Smith, Chem. Phys. Lett. **144**, 563 (1988).

[5] S. Willitsch, M. T. Bell, A. D. Gingell, S. R. Procter, and T. P. Softley, Phys. Rev. Lett. **100**, 043203 (2008).
[6] J. J. van Leuken, J. Bulthuis, S. Stolte, and J. G. Snijders, Chem. Phys. Lett. **260**, 595 (1996).
[7] A. Gijsbertsen, H. Linnartz, G. Rus, A. E. Wiskerke, S. Stolte, D. W. Chandler, and J. Kłos, J. Chem. Phys. **123**, 224305 (2005).
[8] S. Y. T. van de Meerakker, P. H. M. Smeets, N. Vanhaecke, R. T. Jongma, and G. Meijer, Phys. Rev. Lett. **94**, 023004 (2005).
[9] J. J. Gilijamse, S. Hoekstra, S. Y. T. van de Meerakker, G. C. Groenenboom, and G. Meijer, Science **313**, 1617 (2006).
[10] E. I. Dashevskaya, I. Litvin, A. I. Maergoiz, E. E. Nikitin, and J. Troe, J. Chem. Phys. **118**, 7313 (2003).
[11] E. I. Dashevskaya, I. Litvin, E. E. Nikitin, and J. Troe, J. Chem. Phys. **120**, 9989 (2004).
[12] E. I. Dashevskaya, I. Litvin, E. E. Nikitin, I. Oref, and J. Troe, J. Phys. Chem. A **108**, 8703 (2004).
[13] E. E. Nikitin and J. Troe, Phys. Chem. Chem. Phys. **7**, 1540 (2005).
[14] E. I. Dashevskaya, I. Litvin, E. E. Nikitin, and J. Troe, J. Chem. Phys. **122**, 184311 (2005).
[15] A. G. Wickham, T. S. Stoecklin, and D. C. Clary, J. Chem. Phys. **96**, 1053 (1992).
[16] J. Troe, Ber. Bunsenges. Phys. Chem. **99**, 341 (1995).
[17] E. I. Dashevskaya, I. Litvin, E. E. Nikitin, and J. Troe, Phys. Chem. Chem. Phys. **9**, 1559 (2007).
[18] M. Auzinsh, E. I. Dashevskaya, I. Litvin, E. E. Nikitin, and J. Troe, J. Chem. Phys. **128**, 184304 (2008).
[19] W. L. Meerts and A. Dymanus, J. Mol. Spectrosc. **44**, 320 (1972).
[20] W. L. Meerts, Chem. Phys. **14**, 421 (1976).
[21] A. S. Pine, J. W. C. Johns, and A. G. Robiette, J. Mol. Spectrosc. **74**, 52 (1979).
[22] L. H. Coudert, V. Dana, J.-Y. Mandin, M. Morillom-Chapey, R. Farreng, and G. Guelachvili, J. Mol. Spectrosc. **172**, 435 (1995).
[23] J.-Y. Mandin, V. Dana, L. Regalia, A. Baebe, and P. Von der Heyden, J. Mol. Spectrosc. **187**, 200 (1998).
[24] J. D. Graybeal, *Molecular Spectroscopy* (McGraw-Hill, New York, 1988).
[25] M. G. Tenner, E. W. Kuipers, W. Y. Langhout, A. W. Kleyn, G. Nicolasen, and S. Stolte, Surf. Sci. **236**, 151 (1990).
[26] D. A. Varshalovich, A. N. Moskalev, and V. K. Khersonskii, *Quantum Theory of Angular Momentum* (World Scientific, Singapore, 1988).
[27] M. Mizushima, Phys. Rev. **109**, 1557 (1958).
[28] E. Vogt and G. H. Wannier, Phys. Rev. **95**, 1190 (1954).
[29] M. Auzinsh, E. I. Dashevskaya, I. Litvin, E. E. Nikitin, and J. Troe (to be published).